# The PNR to Relaxor Transition in PSN with nearest neighbor Pb-O divacancies

B.P. Burton, Eric Cockayne, D. Gopman, G. Dogan, and Sarah Hood,
Materials Measurement Lab., NIST, 1 Bureau Drive, Gaithersburg, MD 20899 USA

**Abstract**

In previous work, molecular dynamics simulations based on a first-principles-derived effective Hamiltonian for $Pb_{1-X}(Sc_{1/2}Nb_{1/2})O_{3-X}$ (PSN), with nearest-neighbor Pb-O divacancy pairs, was used to calculate $X_{[Pb-O]}$ vs. T, phase diagrams for PSN with: ideal rock-salt type chemical order; nanoscale chemical short-range order; and random chemical disorder. Here, we show that the phase diagrams should include additional regions in which a glassy relaxor-phase (or state) is predicted. With respect to phase diagram topology, these results strongly support the analogy between relaxors and magnetic spin-glass-systems.

# 1 Introduction

Heterovalent perovskite-based $Pb(B,B')O_3$ relaxor ferroelectrics (RFE) [1,2], such as $Pb(Sc_{1/2}Nb_{1/2})O_3$ (PSN), $Pb(Sc_{1/2}Ta_{1/2})O_3$ (PST), and $Pb(Zn_{1/2}Nb_{1/2})O_3$ (PZN) and, *relaxors* [which have no ferroelectric (FE) ground-state] such as $Pb(Mg_{1/3}Nb_{1/2})O_3$ (PMN) and $Pb(Mg_{1/3}Ta_{1/2})O_3$ (PMT), are technologically important transducer/actuator materials with extraordinary dielectric and electromechanical properties. Chemically disordered PSN exhibits polar nano-regions (PNR) characteristics (more polarizable PNR in a less polarizable matrix) above a normal FE-transition at $T_{FE}$~373K. Chu *et al*. [3] demonstrated that the addition of 1.7 atomic% Pb-O divacancies depresses the FE transition temperature (T), from $T_{FE}$~373K to $T_{FE}$~338K, and broadens the T-range in which PNR properties, *e.g.* frequency dispersion in the dielectric response, are observed. Chu *et al*. also reported similar and more complete results for isostructural PST[4-6]. These results suggest that a sufficient bulk concentration of divacancy pairs, $X_{[Pb-O]}$, will drive the system to a relaxor ferroelectric (RFE) state, with an FE-ground-state, or to a fully relaxor state, without an FE-ground-state, at $X_{[Pb-O]} > X_C$, where $X_C$ is the critical composition at which $T_{FE}$->0K.

Chemical disorder and defects such as Pb-vacancies ($V_{Pb}$) [7], oxygen vacancies ($V_O$) or charge-compensating nearest neighbor (nn) Pb-O divacancy pairs ($V_{Pb-O}$) [8], are sources of local, *random fields* $\langle \boldsymbol{h}_i \rangle$ e.g. [9-11] (angle brackets indicate a simulation box average). Hence, the T vs. X phase diagrams presented here are topologically equivalent to the T vs. $\langle \boldsymbol{h}_i \rangle$ diagrams that are typically drawn for analytical mean-field models of magnetic spin-glass (SG) systems [12-16].

Recent publications by Sherrington [13-16] emphasized an analogy between relaxor ferroelectrics and magnetic SG with ***soft pseudospins*** **($\boldsymbol{\xi}_i$); *i.e*. magnetic spins or ferroelectric displacements with variable magnitudes and arbitrary orientations. Pairwise $\boldsymbol{\xi}_i$-$\boldsymbol{\xi}_j$-interactions in these models are frustrated (random-bond frustration [17]), and the combination of frustration plus quenched chemical disorder [18] are identified as essential constituents of relaxors. The model used here: also has *soft pseudospins*** ($\boldsymbol{\xi}_i$) at each Pb-site; first-, second-, and third-nn $\boldsymbol{\xi}_i$-$\boldsymbol{\xi}_j$-pairwise interactions, plus 4th through 39th-nn $\boldsymbol{\xi}_i$-$\boldsymbol{\xi}_j$-pair dipole-dipole interactions; and at each Pb-site. An analysis of $\boldsymbol{h}_i$ that is based on nn Pb-B-site pairs in an ideal perovskite structure with a random cation configuration [11] indicates a distribution of orientations such that 34% are along <111>-type directions; 21% are <001>-type; 19% are <110>-type; 19% are <113>-type; and 7%

are <000>[11] (weighted by $\langle \boldsymbol{h}_i \rangle$-strength the corresponding percentages are: 29% <111>, 21% <001>, 23% <110>, and 27% <113>). The $\boldsymbol{h}_i$ used for the calculations presented here were calculated as the local field imposed by the whole simulation box. In this model, $\boldsymbol{\xi}_i$-$\boldsymbol{\xi}_j$ pairwise interactions are all FE in character, hence the $\boldsymbol{h}_i$ and [Pb-O]-divacancies are the only sources of frustration; and ideally NaCl-ordered pure PSN is unfrustrated.

Results presented here require changes in the phase diagrams that were presented in [19]. The field that was formerly referred to as the RFE-region in T vs. $X_{[Pb\text{-}O]}$ phase diagrams [19] is now divided into: 1) a PNR-region, in which spatially static but orientationally dynamic PNR (centered on 4-5 nm diameter chemically ordered regions [20]) are embedded in a less polarizable matrix; and 2) a ***relaxor–region*** **in which PNR have more static orientations, and simulations exhibit glassy behavior.** The $T(X_{[Pb\text{-}O]})$-curve [*i.e.* $T(\langle \boldsymbol{h}_i \rangle)$-curve] that divides the PNR-region from the relaxor-region is referred to as $\boldsymbol{T}^*(X_{[Pb\text{-}O]})$**.** Dkhil [21] referred to $\boldsymbol{T}^*$ as "...a local phase transition that gives rise to the appearance of static polar nanoclusters." We reject the phrase "local phase transition," because (strictly) phase transitions only occur in infinite systems, and because our results suggest a weakly first-order transition, however, we do predict a subtle stiffening of PNR-orientations below $\boldsymbol{T}^*$.

In previous simulations[11,19], the presence of $V_{Pb}$ vacancies[7] or $V_{[Pb\text{-}O]}$ divacancies[11,19] in PSN lead to more diffuse FE phase transitions, with broadened dielectric susceptibility peaks; however, the **relaxor-phase** (state?) was not clearly delineated. Here, simulations are used to construct $X_{[Pb\text{-}O]}$ vs. T phase diagrams for PSN with random, perfectly rock-salt ordered, and nano-ordered (NO) cation configurations as in [19]. The NO configuration has 20 NaCl-type ordered clusters (diameter~4-5nm) in a percolating random matrix. Divacancy concentration- and T-ranges for normal paraelectric (PE) and FE-phases, and for "RFE-states", were identified from changes in polarization correlations[22], but the **relaxor-phase** *per se* was not delineated.

# 2 Simulations

## 2.1 The Model Hamiltonian

Simulations were performed using the first-principles based effective Hamiltonian $H_{eff}$ that is described in detail in [11]; it expands the potential energy of PSN in a Taylor series about a high-symmetry perovskite reference structure, including those degrees of freedom relevant to FE phase transitions:

$$H_{eff} = H(\{\boldsymbol{\xi}_i\}) + H(e_{\alpha\beta}) + H(\{\boldsymbol{\xi}_i\},\varepsilon_{\alpha\beta}) + PV + H(\{\boldsymbol{\xi}_i\},\varepsilon_{\alpha\beta},\{V_{Pb\text{-}O}\}) \quad (1)$$

where $\{\boldsymbol{\xi}_i\}$ represents Pb-site centered local polar distortion variables of arbitrary magnitudes and orientations; $H(e \rightarrow \uparrow)$ is a homogeneous strain term; $H(\{\boldsymbol{\xi}_i\},\varepsilon_{\alpha\beta})$ is a strain coupling term; and *PV is* the standard pressure-volume term. The first four terms are sufficient to model pressure- and T-dependent phase transitions in a normal FE perovskite without local fields [23]. The fifth term, $H(\{\boldsymbol{\xi}_i\},\varepsilon_{\alpha\beta},\{V_{Pb\text{-}O}\})$, represents coupling between polar variables and "random" local fields, $\boldsymbol{h}_i$, [11,24,25] from: 1) screened electric fields from the quenched distribution of $Sc^{3+}$ and $Nb^{5+}$ ions ; and 2) by $V_{Pb\text{-}O}$.

As described in [19] all simulations were done with a 40×40×40 MD-supercell, in which each Pb-atom is associated with a local distortion vector, $\boldsymbol{\xi}_i$, that indicates the displacement of lead atom-i from its ideal perovskite position. The effective Hamiltonian in Eqn. (1) was used to derive equations of motion, with an MD time-step of 0.06 picoseconds.

Divacancies are modeled by replacing $40^3 X_{[Pb\text{-}O]}$ randomly selected local distortion variables with fixed dipole moments corresponding to $V_{Pb\text{-}O}$ divacancy pairs (*i.e*. local fields directed, from a Pb-site, along one of the 12 ⟨110⟩-type vectors).

## 2.2 Order Parameters

Curves for the Burns temperatures, $T_B(X_{[Pb\text{-}O]})$, [26] and the FE-transitions, $T_{FE}(X_{[Pb\text{-}O]})$ are identical to those in [19]. Curves for $\boldsymbol{T}^*(X_{[Pb\text{-}O]})$ were located by plotting T-dependent $q_{\xi\xi}(T)$- and $q_{\Delta t}(T)$-curves where: $q_{\xi\xi}$ is the self-overlap order parameter, [27] Eqn. (2); and $q_{\Delta t}$ Eqn. (3), is an autocorrelation function that compares the displacement of atom-i at time-$t$ with atom-i at time-$t+\Delta t$ (typically, $\Delta t$ = 100 MD-snapshots = 6.0 picoseconds).

The idea behind $q_{\Delta t}$ is that a time-sensitive order parameter may be more sensitive than $q_{\xi\xi}$ to the sort of PNR-stiffening referred to by Dkhil: [21]

$$q_{\xi\xi} = (1/N)\Sigma_\iota(\boldsymbol{\xi}_\iota \mathbf{o} \boldsymbol{\xi}_\iota) \qquad (2)$$

$$q_{\Delta t} = (1/N)\Sigma_\iota(\boldsymbol{\xi}_t \mathbf{o} \boldsymbol{\xi}_{t+\Delta t}) \qquad (3)$$

where: N is the number of Pb-sites; summations are over the all Pb-displacements; and the averaging represented by angle brackets is over the last 1000 MD-snapshots in a 3000- or 5000 snapshot series (see below). Within the precision of these simulations, both order parameters yield the same results for $\boldsymbol{T}^*$.

Numerical simulations can not distinguish between crossovers and phase transitions where: crossovers correspond to inflection points in the order-parameter vs T curves; and phase transitions correspond to discontinuities in first- or second- T-derivatives of order-parameters (*i.e*. first-order, or continuous- or critical-transition, respectively [28]). Because the results for random- and NO-cation configurations strongly suggest a (weakly) first-order phase transition, $\boldsymbol{T}^*$ will be referred to as a phase *transition*, and the relaxor will be referred to as a *phase*, but with the caveat that $\boldsymbol{T}^*$ may actually mark a crossover, in which case the relaxor is a *state*.

Order parameter values were calculated from MD-snapshots that were taken every 100 MD time-steps in a series of at least 5000 MD-snapshots (enough snapshots that the order-parameters, are approximately constant for 1000 snapshots). Plotted order-parameter values are averages over the last 1000 MD snapshots in a series.

# 3 Results

Representative results for order-parameter vs. T curves are plotted in Figs. 1, 2 and 3. Corresponding phase diagrams are plotted in Figs. 4. In all these plots, T is normalized by $T^0_{FE}$, the ferroelectric transition temperature ($T_{FE}$) of the pure ideally rock-salt-ordered cation configuration. Vertical lines in Figs. 1, 2, and 3 indicate previously determined [19] values for $T_{FE}$ and $T_B$. ll these Figures: $T_{FE}$ is plotted as a solid line (blue online); $T_B$ is plotted as a dashed line (blue online); and $\boldsymbol{T}^*$ is plotted as dotted lines (red online). In Figs. 4, large asterisk-symbols indicate points at which $\boldsymbol{T}^*$ was located in $q_{\xi\xi}(T)$- and $q_{\Delta t}(T)$-curves.

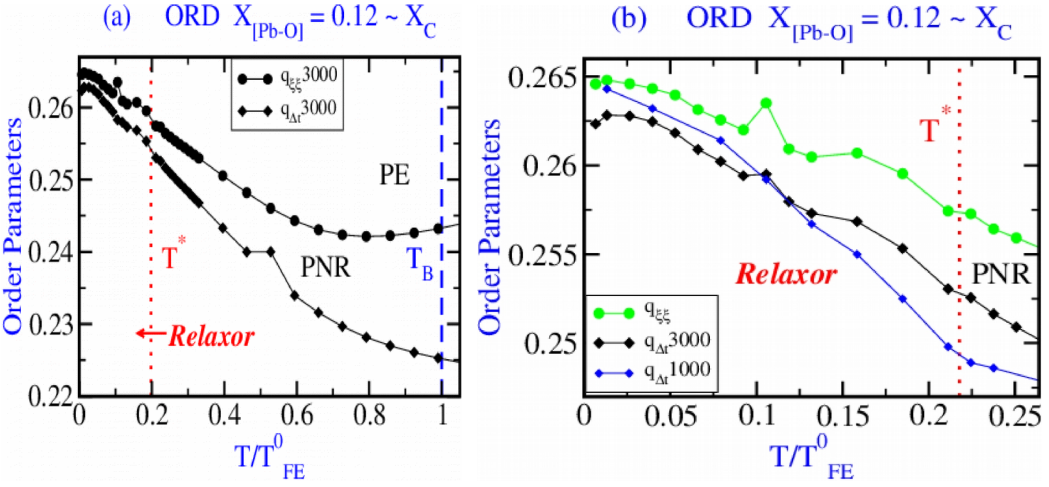


Figure 1: Order parameters that were used to define the relaxor-region in , with ideal rock-salt type Sc:Nb-chemical order: $q_{\xi\xi}$ is the self-overlap order parameter (Eqn. 2); and $q_{\Delta t}$ (Eqn. 3) is a temporal autocorrelation function (1000 and 3000 are results from 1000- and 3000-snapshots, respectively). Panel: (a) is the full diagram; (b) is an enlargement of the low-T portion of the diagram. Here, $\boldsymbol{T^*}$ looks as though it may mark a continuous transition, or a crossover.

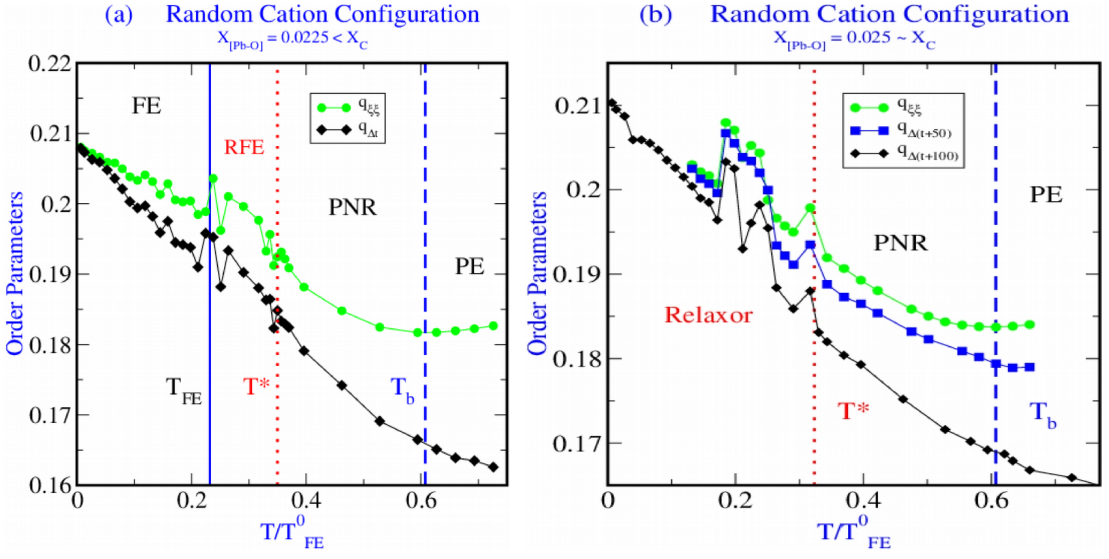


Figure 2: Order parameters as functions of temperature for $Pb1\text{-}X(Sc_{1/2}Nb_{1/2})O_{3\text{-}X}$ with a random Sc:Nb-cation configuration. $q_{\xi\xi}$ and $q_{\Delta t}$ (defined in Eqns.2 and 3): (a) $X_{[Pb-O]}=0.0225<X_C$ where there is a relaxor ferroelectric (RFE) with an FE-ground-state; (b) $X_{[Pb-O]}=0.025\sim X_C$ has no FE-ground-state. In both (a) and (b), $\boldsymbol{T^*}$ appears to mark a weakly first-order transition (an ≈3% discontinuity). In (b) , $q_{\xi\xi}(T)$, $q_{\Delta+50}(T)$, and $q_{\Delta+100}(T)$ exhibit only small quantitative differences.

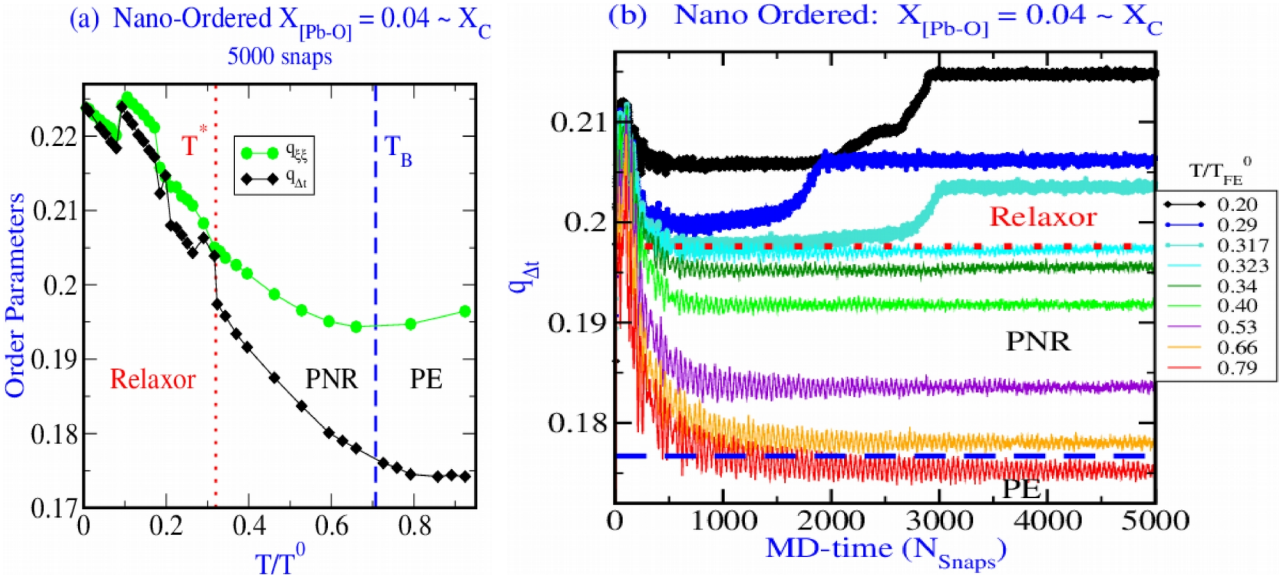


Figure 3: Order parameters as functions of temperature for a nano-ordered Sc:Nb-cation configuration of Pb1-X($Sc_{1/2}Nb_{1/2}$)$O_{3-X}$ with 25% ordered regions in a random matrix: (a) $\boldsymbol{T^*}$ appears to mark a weakly first-order phase transition (an ≈1% discontinuity in $q_{\xi\xi}$ or ≈2% in $q_{\Delta t}$); (b) is a plot of $q_{\Delta t}$ as a function of time, where $N_{snaps}$ is the number of snapshots in a 5000 snapshot series. At $\boldsymbol{T^*}$, above the horizontal dotted line (red online), the system traverses local minima before converging (sticking in a local minimum?).

With decreasing T, $q_{\xi\xi}(T)$ and $q_{\Delta t}(T)$ typically exhibit: broad minima at or near $T_B$; smooth monotonic increase in the PNR-region between $\boldsymbol{T^*}$ and $T_B$; and erratic increase in the relaxor-region below $\boldsymbol{T^*}$. The erratic characters of $q_{\xi\xi}(T)$- and $q_{\Delta t}(T)$-curves in the relaxor-regions of random- and NO-cation-configurations are interpreted as indicating glassy behavior. In particular, Figs 3b, which shows the MD time-dependence of $q_{\Delta t}(T)$ indicates that in the PNR-region above $q_{\Delta t}(T)$ evolves monotonically, however, in the relaxor-region below $\boldsymbol{T^*}$, $q_{\Delta t}(T)$ passes through local minima before finding what we take to be its final value; as one expects for a glassy material.

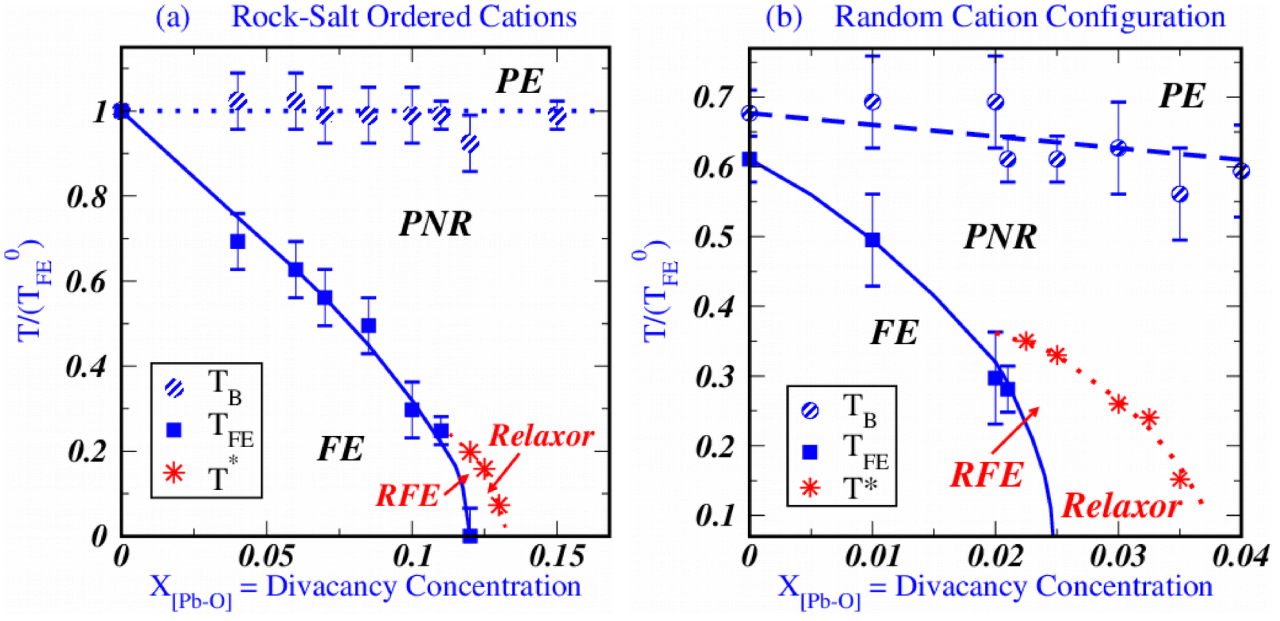

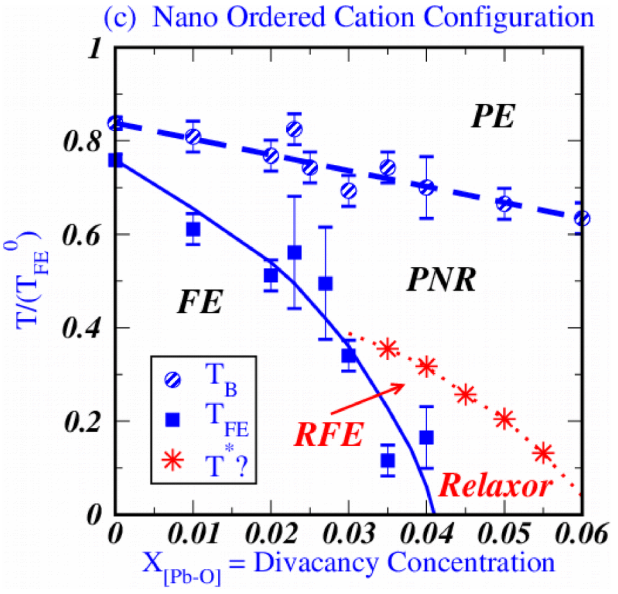


Figure 4: Calculated X[Pb-O] vs T phase diagrams for the system $Pb_{1-X}(Sc_{1/2}Nb_{1/2})O_{3-X}$, with: a) ideal rock-salt type Sc:Nb-chemical order; b) a random Sc:Nb-cation configuration; c) a nano-ordered Sc:Nb-cation configuration, with ordered regions in a random matrix (25% ordered regions that are **≈4–5 nm in diameter**). Labels: PE indicates a normal paraelectric; PNR indicates a system in which chemically ordered regions, with few $h_i$, have higher polarization than the random $h_i$-rich matrix; FE indicates a ferroelectric ground-state; RFE indicates a relaxor-region above the FE-ground-state. Dashed lines (blue online) indicate Burns temperatures (T). Solid lines (blue online) indicate FE to PNR, or FE to RFE transitions. Dotted lines with large asterisk-symbols (red online) indicate $T^*$ (T) the FE to PNR, or relaxor to PNR transitions (crossovers).

## 3.1 Ideal Rock-Salt Chemical Order

Unlike the random- and nano-ordered cation configurations, the PNR to relaxor *transition* is subtle (maybe undetectable) in the ideally NaCl-ordered system; in which [Pb-O]-divacancies are the only source of *random fields*, Figs. 1. All three curves in Figs. 1 exhibit changes in slope at about $T^*=T/T^0_{FE}\sim0.22$, but these changes are smaller and less well defined than those in Figs. 2 and 3; suggesting that $T^*$ may mark either a continuous PNR to relaxor transition, or a crossover. Also, the erratic variations of order parameters, below $T^*$ that are evident in Figs. 2 and 3, are either undetectable within MD-precision, or absent in the NaCl-ordered system.

## 3.2 Random Chemical Disorder and the Nano-Ordered Configuration

Results for the random- and nano-ordered configurations exhibit very similar systematics for $q_{\xi\xi}$(T)- and $q_{\Delta t}$(T)–curves with decreasing T: near $T_B$, there is typically a broad minimum; between $T_B$ and $T^*$, they increase smoothly and monotonically; at $T^*$, there appears to be a (weakly) first-order transition, Figs. 2 and 3; and below $T^*$, they vary erratically, and $q_{\Delta t}$(T) evolves through local minima, Fig. 3b, before converging, or sticking in a local minimum. Also, there are strong correlations between chemical- and polar-order, as reported in Burton *et al*. [19].

# 4 Discussion

## 4.1 Phase Diagram Topology

Notwithstanding the differences between $q_{\xi\xi}$(T)- and $q_{\Delta t}$(T)–curves for the NaCl-ordered configuration vs. those for the random- and NO-ordered configurations, all three phase diagrams exhibit the same topology, Figs. 4. Given that $X_{[Pb-O]}$ and $\langle h_i \rangle$ are interchangeable variables, the phase diagram topology exhibited in Figs. 4 can be taken as a prototype for $Pb(B,B')O_3$ relaxor systems; as depicted in Fig.5. In Figs. 4, the **relaxor field** only

occupies a narrow $X_{[Pb\text{-}O]}$-range from about $X_C$-0.015 to about $X_C$+0.025; *i.e.* a limited range of average $\langle h_i \rangle$-strength. This is the same phase diagram topology that the Sherrington-Kirkpatrick model [12] predicts when the mean exchange, $J_0$, is proportional to x and standard deviation **scaling is as in reference [29]**.

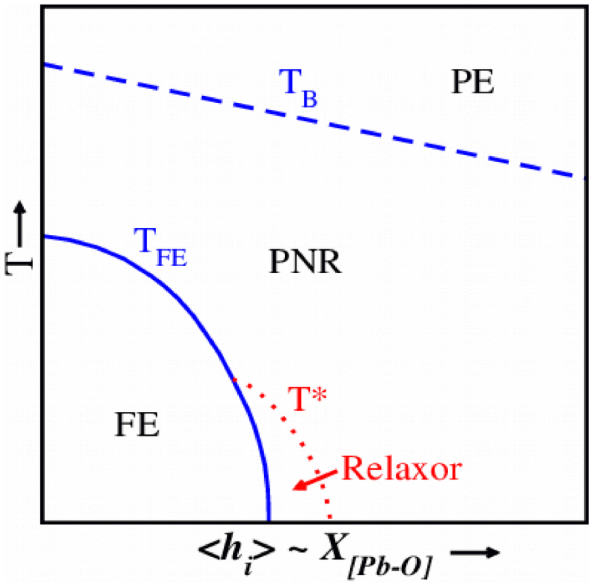


Figure 5: Schematic prototype vs. T phase diagram for relaxor systems.

## 4.2 Comparison With Experiment

Given the approximations in this model, we do not expect *quantitative* accuracy in the calculated phase diagrams, but our results for a random cation configuration (Fig. 4b) agree reasonably well with experimental data of Chu et al. [3]. Their dielectric **permittivity** measurements of ε'(T) and ε"(T) for almost stoichiometric PSN [$Pb_{0.998}(Sc_{1/2}Nb_{1/2})O_{2.998}$], and for PSN with $X_{[Pb\text{-}O]}$=0.17(0.003) [$Pb_{0.983}(Sc_{1/2}Nb_{1/2})O_{2.983}$], respectively, indicate that the former exhibits a first order PNR to FE phase transition, while the latter, $Pb_{0.983}(Sc_{1/2}Nb_{1/2})O_{2.983}$, appears to exhibit fully relaxor behavior without a FE ground state. From Fig. 4b one correctly predicts the PNR to FE phase transition in the $Pb_{0.998}(Sc_{1/2}Nb_{1/2})O_{2.998}$-sample, but one would expect the $Pb_{0.983}(Sc_{1/2}Nb_{1/2})O_{2.983}$-sample to also have a FE-ground-state, with an intermediate RFE-phase. In Fig. 4b, the calculated critical composition, beyond which there is no FE-ground state, is $X_C$~0.024. This is at least half a percent larger than $Pb_{0.983}(Sc_{1/2}Nb_{1/2})O_{2.983}$ (the apparent *maximum* experimental value), which suggests that our model systematically underestimates the strength of random fields from charge disorder, vacancies, or both.

## 4.3 The PNR to relaxor transition and criticality

The apparent predictions of weakly first-order PNR to relaxor transitions in the random- and nano-ordered cation configurations has an important implication for relaxors. Specifically, a weakly first-order transition implies proximity to a critical point, and this suggests a simple explanation for the extraordinary electro-mechanical properties that are observed in relaxors; *i.e.* these properties diverge at a critical point, and are significantly enhanced close to a critical point. Indeed, Kutnjak *et al.*[30] attributed the giant electromechanical response in PMN-PT to a liquid-vapor like critical point. The results reported here suggest that the PNR to relaxor transition is *typically* close to a critical point; e.g. *close*, in the sense that the application of a modest electrical field can drive the system from weakly first-order to critical.

## 4.4 Additional Phase Transitions?

In $Eu_XSr_{1-X}$ the experimental phase diagram exhibits a ferromagnetic to SG transition,[31] and in $Fe_{1-X}Au_X$ there are ferromagnetic to Mixed-phase- and SG to Mixed-phase-transitions [32] (the Mixed-phase is ferromagnetic but replica-symmetry breaking (RSB) [27]); i.e. a spin glass phase without ferromagnetism (ferroelectricity), that is dynamically glassy. Compelling evidence of analogous transitions was not detected in this work [33], but such transitions are not ruled out, and there is clear similarity between relaxor- and magnetic- spin-glass phase diagrams: Fig. 5 and Table I.

Table 1: Relaxor vs. Magnetic Spin-Glass Analogy.

| *Relaxor* | *Magnetic Spin−Glass* |
|---|---|
| *PE=paraelectric* | *PM=paramagnetic* |
| *PNR=Polar Nano Regions* | *SPM=superparamagnetic* |
| *FE=Ferroelectric* | *FM=Ferromagnetic* |
| *RSB=Replica−Symmetry−Breaking?* | *RSB* |
| ***relaxor*** | *SG=SpinGlass* |

## 5 Conclusions

The phase diagrams presented in Burton *et al*. [19] were incomplete because they omitted $T^*(X)$-curves; *i.e*. delineation of the **relaxor-phase** field as a subspace of the PNR-field. Results presented here: include: a calculations of $T^*(X)$-curves; suggest a prototype relaxor phase diagram topology; and strongly support the analogy between relaxors and magnetic spin-glasses, Table I.

The combination of soft-spins with explicit 1šț-3řd nn-pairwise pseudospin-pseudospin interactions, plus 4ťh-39ťh nn dipole-dipole interactions, and random fields from both chemical disorder and Pb-O nn-divacancies, is evidently sufficient to model perovskite based heterovalent $Pb(B,B')O_3$ relaxor systems. Both the self-orvelap order parameter and the autocorrelation function appear to be good order parameters for locating **$T^*(X)$- or $T^*(\langle h_i \rangle)$-curves, and for demonstrating the glassy character of the relaxor-phase, which only occupies a narrow range in $X_{[Pb\text{-}O]}$, or equivalently in $\langle h_i \rangle$**.

Previous conclusions [19,20] about the strong correlation between chemically ordered regions and PNR are reinforced, with the addition that the orientations of PNRs become more static in the relaxor region, below the PNR to relaxor transition. In the random- and nano-ordered cation configurations, there appears to be a weakly first-order transition at $T^*$, but results for the rock-salt ordered configuration are suggestive of a continuous transition or a crossover. Chemical inhomogeneities such as chemical short-range order, apparently amplify relaxor character.

## References


[1] G.A. Smolensky and A.I. Agranovskaya, Sov. Phys. Sol. State 1, 1429 (1959).

[2] L. E. Cross, Ferroelectrics 76, 241 (1987).

[3] F. Chu, I.M. Reaney and N. Setter, J. Appl. Phys. 77[4], 1671 (1995).

[4] F. Chu, N. Setter and A. K. Tagantsev, J. Appl. Phys. 74[8], 5129 (1993).
[5] F. Chu, I.M. Reaney and N. Setter, J. Amer. Ceram. Soc. 78[7], 1947 (1995)
[6] F. Chu, G. Fox and N. Setter, J. Amer. Ceram. Soc. 81, (6) 1577 (1998)
[7] L. Bellaiche, J. Ìñguez, E. Cockayne, and B. P. Burton Phys. Rev. B 75, 014111 (2007).
[8] E. Cockayne and B. P. Burton, Phys. Rev. B 69, 144116 (2004).
[9] W. Kleemann, J. Dec, V. V. Shvartsman, Z. Kutnjak and T. Braun, Phys. Rev. Lett. 97 065702 (2006).
[10] J. Adv. Dielectrics V2, No. 2 1241001 (2012).
[11] B. P. Burton, E. Cockayne, S. Tinte and U. V. Waghmare, Phase Trans. 79, 91 (2006).
[12] D. Sherrington and S. Kirkpatrick Phys. Rev. Lett. 35, 1792 (1975).
[13] D. Sherrington Phys. Rev. Lett. 111, 227601 (2013).
[14] D. Sherrington Phys. Rev. B 89, 064105 (2014).
[15] D. Sherrington Physica Status Solidi b 251, 1967 (2014).
[16] D. Sherrington Phase Transitions 88, 202 (2015).
[17] S.F. Edwards, P.W. Anderson, J. Phys. F 5 965 (1975).
[18] The phrase "quenched chemical disorder" implies that the chemical configuration is fixed within the temperature range that polar order-disorder is analyzed.
[19] B. P. Burton, E. Cockayne, S. Tinte and U. V. Waghmare, Phys. Rev. B 77, 144114 (2008).
[20] B.P. Burton, E. Cockayne, and U.V. Waghmare, Phys. Rev. B 72, 064113 (2005).
[21] B. Dkhil, P. Gemeiner, A. Al-Barakaty, L. Bellaiche, E. Dulkin, E. Mojaev, and M. Roth, Phys. Rev. B 80 064103 (2009).
[22] S. Tinte, B. P. Burton, E. Cockayne and U. V. Waghmare, Phys. Rev. Lett. **97**, 137601 (2006).
[23] W. Zhong, D. Vanderbilt and K. M. Rabe, Phys. Rev. Lett. **73**, 1861 (1994); K. M. Rabe and U. V. Waghmare, Phys. Rev. B **52**, 13236 (1995); U. V. Waghmare and K. M. Rabe, Phys. Rev. B **55**, 6161 (1997).
[24] U. V. Waghmare, E. Cockayne, and B. P. Burton, Ferroelectrics 291, 187 (2003).
[25] B. P. Burton, U. V. Waghmare and E. Cockayne, TMS Letters, 1, 29 (2004).
[26] G. Burns and F. H. Dacol, Solid State Commun. 48, 853 (1983).
[27] T. Castellani and A. Cavagna J. Stat. Mecha. P05012 (2005) PII: S1742-5468(05)99356-4
[28] Fisher, M E (1998) Renormalization group theory: its basis and formulation in statistical physics, Reviews in Modern Physics 70(2) 653-681.
[29] D. Sherrington, Private communication.
[30] Z. Kutnjak, J. Petzelt and R. Blinc Nature 441 956 (2006).
[31] H. Maletta and P. Convert, Phys. Rev. Lett. 42, 108, (1979)
[32] R.B. Coles, B. Sarkissian, and R.H. Taylor, Phil. Mag. B37, 489 (1978)
[33] The strongest suggestion of such a transition is in the NO configuration where q✎$_t$(T) exhibits a low-T reduction to a plateau, which does not seem to define a consistent phase-boundary or crossover.